SUPPLEMENTAL MATERIAL

Nodosome inhibition as a novel broad-spectrum antiviral strategy against arboviruses, enteroviruses and SARS-CoV-2

Daniel Limonta, Lovely Dyna-Dagman, William Branton, Valeria Mancinelli, Tadashi Makio, Richard W. Wozniak, Christopher Power, Tom C. Hobman

Cells and viruses. The prototype Zika virus (ZIKV) strain isolated in Puerto Rico (PRVABC-59) in 2015 (1) was kindly provided by the National Microbiology Laboratory of Canada (Winnipeg, Canada). Dengue virus-2 (DENV-2, 16681 strain) clone was provided by Dr. Bart Bartenschlager at the Heidelberg University Hospital (Heidelberg, Germany). Mayaro virus (MAYV, TRVL 15537) strain was obtained from ATCC. Arboviruses were propagated in *Aedes albopictus* C6/36 cells grown in MEM (Thermo Fisher Scientific) supplemented with 10% fetal bovine serum (Thermo Fisher Scientific), L-glutamine, Penicillin-Streptomycin and MEM non-essential amino acids at 32°C.

Arbovirus stocks were prepared after inoculating C6/36 cells using a multiplicity of infection (MOI) of 0.2 and then harvesting cell culture media between 24 to 96 hours post-infection. Virus-containing media were clarified by centrifugation at 3200 x g for 10 minutes. Human fetal astrocytes (HFAs) were prepared as previously described (2). Briefly, human fetal brain tissues were obtained from 15 to 19-week aborted fetuses. After isolation of astrocytes, cells were split, and all experiments were conducted with cells between the fifth and seventh passages. HFAs were grown in MEM supplemented with 10% fetal bovine serum, 15 mM HEPES (Thermo Fisher

Scientific) L-glutamine, MEM non-essential amino acids, sodium pyruvate, and 1g/mL glucose. Vero cells (ATCC, CCL-81) were maintained in DMEM (Thermo Fisher Scientific) supplemented with 10% fetal bovine serum, 15 mM HEPES, L-glutamine and Penicillin-Streptomycin. Stocks of the Faulkner strain of coxsackievirus B5 (CBV5) were prepared in MA104 cells (ATCC) by the Department of Laboratory Medicine & Pathology at the University of Alberta.

Severe acute respiratory syndrome coronavirus 2 (SARS-CoV-2/CANADA/VIDO 01/2020) was kindly provided by Dr. Darryl Falzarano (Vaccine and Infectious Disease Organization-International Vaccine Centre, University of Saskatchewan, Canada). SARS-CoV-2 strain was propagated in Vero-E6 cells (ATCC) grown in DMEM supplemented with 10% fetal bovine serum, 15 mM HEPES, L-glutamine and Penicillin-Streptomycin.

A549, Huh7, U251 (ATCC) and ACE2-hyperexpressing SK-N-SH cells were maintained in DMEM while HEL-18 human primary embryonic pulmonary fibroblasts (3) were maintained in RPMI 1640 (Thermo Fisher Scientific) medium supplemented with 10% fetal bovine serum, 15 mM HEPES, L-glutamine and Penicillin-Streptomycin.

Generation of ACE2-SK-N-SH cells. SK-N-SH cells stably expressing ACE2 were constructed using lentivirus transduction (4, 5). The coding region of the human ACE2 gene from the plasmid hACE2 (Addgene plasmid #1786) (6) was subcloned into the lentiviral vector pLenti-puro (Addgene plasmid #39481) (7) to generate pLenti-ACE2. Next, lentiviral pseudoparticles were harvested from the media of HEK293T cells (ATCC) transfected with viral packaging vectors (5) and pLenti-ACE2 using Lipofectamine 3000 (Invitrogen). SK-N-SH cells (ATCC) were transduced with the lentiviral pseudoparticles and stably transduced cells were selected using 10 μg/mL puromycin in DMEM containing 10% FBS. Expression of ACE2 protein was confirmed by western blotting using anti-ACE2 antibodies (R & D Systems).

Viral infections of cells. Cells were seeded in 96-wells plates (Greiner) at 1-1.5 x 10^4 cells per well. The next day, cells were rinsed once with PBS and viruses at an MOI of 0.05 to 5 were added to the wells. Cells were then incubated for 1 (SARS-CoV-2) or 2 (arboviruses and CVB5) hours at 37°C using fresh media supplemented with 3% fetal bovine serum. Next, the inoculum was removed, and the cells were washed twice with PBS. Complete culture medium was added to each well, and cells were incubated at 37°C and 5% CO_2. Mock-infected cells were incubated with the culture supernatant from uninfected cells.

Cellular RNA purification, cDNA synthesis, and qRT-PCR. Total RNA was extracted from cultured cells using NucleoSpin RNA (Macherey-Nagel GmbH & Co) kits. Samples were then treated with RNase-free DNase (Macherey-Nagel GmbH & Co) before a portion (0.5-1 µg total RNA) was subjected to reverse transcription using ImProm-II Reverse Transcriptase (Promega). Cellular transcripts and viral RNA were quantitated by qRT-PCR using PerfeCTa SYBR Green SuperMix (Quanta BioSciences) in a CFX96 Touch Real-Time PCR Detection System instrument (Bio-Rad) under the following cycling conditions: 40 cycles of 94°C for 30 s, 55°C for 60 s, and 68°C for 20 s. Gene expression (fold change) was calculated using the $2^{(-\Delta\Delta CT)}$ method with human β-actin mRNA transcript as the internal control.

The following forward and reverse primer pairs were used for PCR:

Primer name	Sequence
β-actin	5'-GGATCAGCAAGCAGGAGTATG-3' 5'-GCATTTGCGGTGGACGAT-3'

NOD2 (nucleotide-binding oligomerization domain-containing protein 2)	5’-TCTCTGTGCGGACTCTACTC-3’ 5’-ATCCGTGAACCTGAACTTG-3’
RSAD2 (radical SAM domain-containing 2 or viperin)	5’-CTTTTGCTGGGAAGCTCTTG-3’ 5’-CAGCTGCTGCTTTCTCCTCT-3’
GSDMD (gasdermin D)	5’-GTGTGTCAACCTGTCTATCAAGG-3’ 5’-CATGGCATCGTAGAAGTGGAAG-3’
Casp1 (caspase 1)	5’-TCACTGCTTCGGACATGACTACA-3’ 5’-GGAACGTGCTGTCAGAGGTCTT-3’
GBP5 (guanylate binding protein 5)	5’-TCCTCGGATTATTGCTCGGC-3’ 5’-CCTTTGCGCTTCAGCCTTTT-3’
NLRC5 (NOD-like receptor family CARD domain containing 5)	5’-TGGGAAGACACTCAGGCTAA-3’ 5’-ATCATCGTCCTCACAGAGGTT-3’
IL-18 (Interleukin-18)	5’-GACTGTAGAGATAATGCAC-3’ 5’-CTTCGTTTTGAACAGTGAAC-3’
NLRP1 (NLR Family Pyrin Domain Containing 1)	5’-ACCATGGTAGTCCTGTTCAG-3’ 5’-GCGAGTTTCCACTTAGGTC-3’
ASC (apoptosis-associated speck like protein containing a caspase recruitment domain)	5’-GCACTTTATAGACCAGCACCG-3’ 5’-CTGAAGAGCTTCCGCATCTTG-3’
IL-1 β (Interleukin-1 β)	5’-AACCTCTTCGAGGCACAAGG-3’ 5’-GTCCTGGAAGGAGCACTTCAT-3’

EIF2AK2 (eukaryotic translation initiation factor 2-alpha kinase 2)	5’-ACCTCAGTGAAATCTGACTACC-3’ 5’-CAGATGATGATTCAGAAGCG -3’
IFI-16 (gamma-interferon-inducible protein 16)	5’-ACAAACCCGAGAAACAATGACC-3’ 5’-GCATCTGAGGAGTCCGAAGA-3’
NLRC4 (NOD-like receptor family CARD domain containing 4)	5’-CTGAGCAGCCTGTTGAAAC-3’ 5’-CATCCATCACTGCTCACAC-3’
NLRP3 (NLR family pyrin domain containing 3)	5’-CCAAGAATCCACAGTGTAACC-3’ 5’-CTTCACAGAACATCATGACCC-3’
OAS-1 (2'-5'-oligoadenylate synthetase 1)	5’-TTCTTAAAGCATGGGTAATTC-3’ 5’-GAAGGCAGCTCACGAAAC-3’
MX2 (Myxovirus resistance protein 2 or interferon-induced GTP-binding protein MX2)	5’-CAGCCACCACCAGGAAACA-3’ 5’-TTCTGCTCGTACTGGCTGTACAG-3’
ZIKV (8)	5’-CCTTGGATTCTTGAACGAGGA-3’ 5’-AGAGCTTCATTCTCCAGATCAA-3’
DENV (9)	5’-TTGAGTAAACTGTGCAGCCTGTAGCTC-3’ 5’-GGGTCTCCTCTAACCTCTAGTCCT-3’
MAYV (10)	5’-AAGCTCTTCCTCTGCATTGC-3’ 5’-TGCTGGAAACGCTCTCTGTA-3’
CVB5 (11)	5’-ACACGGACACCCAAAGTAGTCGGTTCC-3’ 5’-TCCGGCCCCTGAATGCGGCTAATCC-3’
SARS-CoV-2 (12)	5’-CAATGGTTTAACAGGCACAGG-3’ 5’-CTCAAGTGTCTGTGGATCACG-3’

Viral titer assay. Flaviviruses and alphaviruses were serially diluted (10-fold dilutions) and monolayers of Vero CCL-81 cells at 37 °C were infected for 2 hours. For the SARS-CoV-2 plaque assay, Vero-E6 cells were infected for 1 hour in a biosafety level 3 laboratory of the University of Alberta. The monolayers were overlaid with a mixture of MEM (Thermo Fisher Scientific) and 0.75-1.5% carboxymethylcellulose (Sigma-Aldrich) following infection. The cells were maintained at 37 °C for 2-7 days, depending on the virus (2 days for MAYV, 3 days for SARS-CoV-2, 4 days for ZIKV, and 7 days for DENV-2) for plaque development. Cells were fixed with 10% formaldehyde and stained with 1% crystal violet in 20% ethanol after which plaques were counted.

Cytotoxicity assays. The CellTiter-Glo Luminescent Cell Viability Assay (Promega) was used for quantitation of ATP in cultured cells. Cell lysates were assayed after mixing 100 µl of complete media with 100 µl of reconstituted CellTiter-Glo Reagent (buffer plus substrate) following the manufacturer's instructions. Samples were mixed by shaking the plates after which luminescence was recorded with a GloMax Explorer Model GM3510 (Promega) 10 min after adding the reagent.

Antiviral drug assays. Unless otherwise indicated, cells were cultured in 96-well plates (Greiner) and viral replication and titers were determined by qRT-PCR on total RNA extracted from cells and plaque assay of cell supernatants respectively. Cells seeded into 96-well plates (Greiner) at 1-1.5 x 10^4 cells per well were infected the next day with ZIKV, DENV-2, MAYV, CVB5 or SARS-CoV-2 (MOI=0.05-5) followed by treatment with 5, 10, 20 and 40 µM of GSK717 (13) (Sigma-Aldrich) or an equal volume of DMSO. Viral replication and titers were determined 24 to 72-hours post-infection.

HFAs (5 x 10^4 cells per well) were grown in 24-well plates (Greiner) and after ZIKV infection (MOI=0.05-5), GSK717 (5-40 µM) was added to carry out a 3-day kinetics of viral titers. For some

drug assays, an MOI of 1.0 was used to infect A549 cells on coverslips with ZIKV, DENV-2 or MAYV at 1 x 10^5 cells per well in 12-well plates (Greiner) for indirect immunofluorescence of viral antigens. For time-of-addition drug assays, nodosome inhibitors or DMSO were added either immediately or 12 or 24-hours after the virus absorption step. Cell supernatants were collected for viral titer determination at 24, 36, and 48-hours after addition of the compounds.

After infecting A549 cells with ZIKV, DENV-2, CVB5 or MAYV (MOI=0.05-5), cells were treated with the RIPK2 inhibitor GSK583 (14) (Sigma-Aldrich) or DMSO as control for 24 hours. Furthermore, a time-of-addition assay, as described above, was performed. Cell supernatants, cells on coverslips and total cellular RNA were collected for determining viral titers by plaque assay, percentage of infected cells by indirect immunofluorescence and viral replication by qRT-PCR respectively.

GSK717 or GSK583 were used to treat SARS-CoV-2 (MOI=0.05-5) infected ACE2-SK-N-SH cells seeded into 96-well or 12-well-plates, followed by viral RNA quantification, viral titer determination or indirect immunofluorescence as described above for the arbovirus inhibition assays. The selectivity index (SI) for each drug was calculated by dividing the 50% cytotoxic concentration (CC_{50}) by the 50% inhibitory concentration (IC_{50}).

To determine if/how GSK583 and GSK717 affected host cell antiviral signaling, A549 cells seeded into 96-well plates (Greiner) at 1.5 x 10^4 cells per well were treated with drugs or DMSO alone for 16 hours. The cells were then treated with human recombinant IFN-α (100U/mL) or transfected with poly(I:C) (0.2 μg/well) using TransIT (0.3 μL/well, Mirus Bio LLC). At the 4- and 8-hour time points, total cellular RNA was collected for ISGs quantitation by qRT-PCR.

As a positive control of the flaviviral inhibition in infected A549 cells (MOI=0.5-5), we used the anti-flavivirus nucleoside analog NITD008 (15) (Sigma-Aldrich) at 0.75-3 µM or DMSO alone (data not shown). In the SARS-CoV-2 inhibition assays, remdesivir (16) (MedKoo Biosciences, Inc.) in infected Vero E6 cells (MOI=0.1) was used as positive control at 0.1-10 µM or DMSO as vehicle (data not shown).

Immunoblotting. A549 cells were seeded in 6-wells plates (2 x 10^5 cells per well) and then infected the next day in the presence or absence of GSK583 or DMSO alone for 24 hours. Cells were washed three times with PBS before lysing with SDS Sample buffer containing β-mercaptoethanol (2%) and 1 U of Benzonase (Millipore) per sample. The samples were heated at 98°C for 10 min to denature proteins, separated by SDS-PAGE and then transferred to polyvinylidene difluoride membranes for immunoblotting as described previously (17). RIPK2 protein was detected with 1:1000 anti-RIPK2 antibody (Abcam, ab8428). ZIKV capsid protein was detected with 1:1000 rabbit anti-ZIKV. Membranes were incubated overnight at 4°C with the primary antibodies. After three washes with Tris-buffered saline containing Tween, membranes were incubated for 1 hour at room temperature with secondary antibodies (Invitrogen) diluted 1:10000 anti-rabbit Alexa Fluor 700. Lastly, blots were imaged and analyzed using the Odyssey CLx imaging system and Image Studio software 5.2 (LI-COR Biosciences) respectively.

Immunostaining and imaging. Cells on coverslips were processed by fixing for 15 min at room temperature with 4% paraformaldehyde in PBS. Cells were washed three times in PBS and then permeabilized/blocked in Blocking buffer with 0.2% Triton-X100 and 3% BSA in PBS for 1 hour at room temperature followed by washing with PBS containing 0.3% BSA. Incubations with primary antibodies diluted 1:500 (mouse anti-Flavivirus Group Antigen 4G2, Millipore), 1:200 (rabbit monoclonal anti-chikungunya capsid kindly donated by Dr. Andres Merits at University of

Tartu, Estonia), or 1:250 (mouse monoclonal anti-spike SARS-CoV/SARS-CoV-2, GenTex) in Blocking buffer were carried out at room temperature for 1.5 hour followed by three washes in Washing buffer (0.02% Triton-X100 with 0.3% BSA and PBS).

Samples were then incubated with secondary antibodies (1:1000) in Blocking buffer containing 1 µg/mL of DAPI for 1 hour at room temperature followed by three washes in Washing buffer. Secondary antibodies (Invitrogen) were Alexa Fluor 488 anti-mouse or Alexa Fluor 647 anti-rabbit. Confocal images of cells on coverslips were acquired using an Olympus 1x81 spinning disk confocal microscope (Tokyo, Japan) and images were analyzed using Volocity 6.2.1 software. A set of confocal imaging was acquired using a Cytation 5 Cell Imaging Multi-Mode Reader and analyzed using Gen5 software (Biotek). Total and antigen-positive cells were counted in 10 image fields per well, and the percentage of infected cells was obtained.

Supplemental Figure legends

Fig S1. Inflammasome induction by human recombinant IFN-α and NOD2 silencing in HFAs. HFAs were treated with human recombinant IFN-α for 4, 8 and 12 hours after which relative expression of inflammasome genes gasdermin D (*GSDMD*) (**A**), caspase 1 (*Casp1*) (**B**), guanylate binding protein 5 (*GBP5*) (**C**) and NOD-like receptor family CARD domain containing 5 (*NLRC5*) (**D**) were determined. (**E**) HFAs were transfected with *NOD2*-specific or non-silencing siRNAs for 24-hours followed by ZIKV infection (MOI=0.05). Total cellular RNA was collected at 48 hours post-infection for *NOD2* gene quantitation by qRT-PCR. Relative levels to mock of *NOD2* are shown. (**F**) Cellular ATP levels in uninfected HFAs were determined using the CellTiter-Glo assay kit after *NOD2* silencing for 72 hours. Values are expressed as the mean of

three independent experiments. Error bars represent standard errors of the mean. *$P < 0.05$, **$P < 0.01$, and ***$P < 0.001$, by the Student *t* test.

Fig S2. NOD2 blocking drug GSK717 displays anti-ZIKV activity in different cell types. Human primary embryonic pulmonary fibroblasts (HEL-18) were treated with GSK717 or DMSO as control for 72 hours after ZIKV infection with MOI of 0.05 and 5. ZIKV titers are shown as relative fold with MOI of 0.05 (**A)** and 5 (**B**) at 48-72 hours post-infection and as PFU/mL with MOI of 0.05 (**C**) at 48 hours post-infection. (**D**) Cellular ATP levels in uninfected HEL-18 after treatment with DMSO or GSK717 for 72 hours are shown. (**E**) Viral titers as relative fold in A549 cells infected with ZIKV (MOI=0.1) for 0, 12 or 24 hours followed by GSK717 drug or DMSO addition for 48, 36 or 24 hours respectively are shown. Values are expressed as the mean of three independent experiments. Error bars represent standard errors of the mean. *$P < 0.05$, **$P < 0.01$, and ***$P < 0.001$, by the Student *t* test.

Fig S3. NOD2 inhibitor GSK717 blocks the spread of multiple arboviruses. (**A**) A549 cells were infected with DENV-2 (MOI=1) followed by treatment with DMSO or GSK717 at 20 or 40 μM for 48 hours before immunostaining for detecting DENV envelope protein. Images were acquired using a spinning disk confocal microscope equipped with Volocity 6.2.1 software. Infected cells were counted in 10 different fields for GSK717 and DMSO treated samples. (**B**) A549 or ACE2-SK-N-SH cells were infected with arboviruses (MAYV or DENV-2) or SARS-CoV-2 respectively (MOI=0.05-5) for 48 hours followed by total cellular RNA collection for quantitation of *NOD2* mRNA. *NOD2* expression values are shown as relative to mock. (**C**) A549 cells were infected with CVB5 (MOI=0.1) after which total cellular RNA were collected at 24- and 48-hours post-infection for *NOD2* expression quantitation by RT-qPCR. Gene expression as

relative to mock is presented. Values are expressed as the mean of three independent experiments. Error bars represent standard errors of the mean. $^{**}P < 0.01$, by the Student *t* test.

Fig S4. RIPK2 inhibitor GSK583 suppresses arboviral replication. A549 cells were infected with MAYV (MOI=0.1) and treated with RIPK2 inhibitor GSK583 (30 μM) or DMSO. Relative fold of titers (**A**) and viral genome (**B**) at 12- and 24-hours post-infection is shown. (**C**) A549 cells infected separately with arboviruses at low MOI (0.05) were treated with GSK583 (7.5-30 μM) or DMSO for 24 hours before supernatant collection for plaque assays. Viral titers as relative fold is shown. Cells were infected with ZIKV (**D**) or MAYV (**E**) at the MOI of 0.1 followed by the addition of GSK583 or DMSO immediately after infection (0 hours) or 24 hours post-infection. Relative viral titers in media were determined 24 hours after the treatment. Values are expressed as the mean of three independent experiments. Error bars represent standard errors of the mean. $^{*}P < 0.05$, $^{**}P < 0.01$, and $^{***}P < 0.001$ by the Student *t* test.

Fig S5. RIPK2 inhibitor GSK583 blocks the spread of arboviruses. (**A**) Representative confocal imaging (20X) of GSK583 effect on MAYV-infected A549 cells. (**B**-**D**) Cells were infected with MAYV, ZIKV or DENV (MOI=1) and then treated with GSK583 (15 or 30 μM) for 24 hours before processing for indirect immunofluorescence. Infected cells were identified using anti-alphavirus capsid (MAYV) or anti-flavivirus envelope 4G2 (ZIKV and DENV-2) and Alexa Fluor 647 anti-rabbit or 488 anti-mouse antibodies. Nuclei were stained with DAPI. Images of MAYV-infected cells were acquired using a Cytation 5 Cell Imaging Multi-Mode Reader and analyzed using Gen5 software (Biotek) while images of flavivirus infected cells (ZIKV and DENV-2) were acquired using a spinning disk confocal microscope with Volocity 6.2.1 software. Infected cells were determined by counting within 10 different fields for each sample of MAYV (**B**), ZIKV (**C**) and DENV-2 (**D**). (**F**) Immunoblotting of RIPK2 in ZIKV-infected A549 cells.

Cells were infected with ZIKV at the MOI of 0.05 and treated with GSK583 or DMSO followed by immunoblot analyses of cell lysates harvested 24 hours post-infection. RIPK2 and ZIKV capsid were detected with rabbit antibodies. Values are expressed as the mean of three independent experiments. Error bars represent standard errors of the mean. *$P < 0.05$, **$P < 0.01$, and ***$P < 0.001$, by the Student *t* test.

Fig S6. RIPK2 inhibitor blocks the infection by and spread of SARS-CoV-2 in ACE2-SK-N-SH. (**A**) ACE2-SK-N-SH were infected with SARS-CoV-2 (MOI=0.1) followed by treatment with 30 μM of GSK583 or DMSO. Cell supernatants were collected at 12- and 24-hours post-infection for plaque assay. Viral titers as PFU/mL are shown. (**B**) The same drug concentration was also added at 0 and 24 hours after infection with SARS-CoV-2 (MOI=0.1) to determine titers (PFU/mL) in ACE2-SK-N-SH supernatants 24 hours post-treatment. (**C**) Representative confocal imaging (20X) of ACE2-SK-N-SH infected with SARS-CoV-2 (MOI=1) and treated with GSK583 or DMSO for 24 hours. After fixation, coronavirus-infected cells were stained using mouse monoclonal antibody to SARS spike protein as primary antibody and secondary antibodies were Alexa Fluor 488 donkey anti-mouse. Nuclei were stained with DAPI. Confocal images were acquired using a spinning disk confocal microscope with Volocity 6.2.1 software. (**D**) Cells were counted in 10 different fields for quantitation of infected cells after GSK583 or DMSO treatment. Values are expressed as the mean of three independent experiments. Error bars represent standard errors of the mean. *$P < 0.05$, **$P < 0.01$, and ***$P < 0.001$, by the Student *t* test.

Fig S7. Nodosome inhibitors enhance the innate immune response. (**A**-**F**) A549 cells were treated with NOD2 inhibitor (GSK717) or RIPK2 inhibitor (GSK583) for 16 hours and then transfected with or without poly(I:C) (0.2 μg/well) using TransIT (0.3 μL/well). Four- and eight-hours post-transfection, total cellular RNA was harvested and subjected to qRT-PCR to determine

relative levels of ISGs (*Casp1, GBP5, NLRC5, NLRP3, NLRC4* and *MX2*) transcripts. (**G**) A549 cells were transfected with poly(I:C) (0.2 μg/well) or (**H**) treated with human recombinant IFN-α (100U/mL) for 4- or 8-hours after which total cellular RNA was subjected to qRT-PCR to determine relative expression of ISGs. Values are expressed as the mean of three independent experiments. Error bars represent standard errors of the mean. **P* < 0.05, and ***P* < 0.01, by the Student *t* test.

SUPPLEMENTAL REFERENCES

1. Lanciotti RS, Lambert AJ, Holodniy M, Saavedra S, Signor Ldel C. 2016. Phylogeny of Zika Virus in Western Hemisphere, 2015. Emerg Infect Dis 22:933-5.
2. Limonta D, Branton W, Wong CP, Saito L, Power C, Hobman TC. 2020. Use of Primary Human Fetal Astrocytes and Tissue Explants as Ex Vivo Models to Study Zika Virus Infection of the Developing Brain. Methods Mol Biol 2142:251-259.
3. Megyeri K, Berencsi K, Halazonetis TD, Prendergast GC, Gri G, Plotkin SA, Rovera G, Gönczöl E. 1999. Involvement of a p53-dependent pathway in rubella virus-induced apoptosis. Virology 259:74-84.
4. Capitanio JS, Montpetit B, Wozniak RW. 2017. Human Nup98 regulates the localization and activity of DExH/D-box helicase DHX9. Elife 6.
5. Schoggins JW, Wilson SJ, Panis M, Murphy MY, Jones CT, Bieniasz P, Rice CM. 2011. A diverse range of gene products are effectors of the type I interferon antiviral response. Nature 472:481-5.

6. Li W, Moore MJ, Vasilieva N, Sui J, Wong SK, Berne MA, Somasundaran M, Sullivan JL, Luzuriaga K, Greenough TC, Choe H, Farzan M. 2003. Angiotensin-converting enzyme 2 is a functional receptor for the SARS coronavirus. Nature 426:450-4.

7. Guan B, Wang TL, Shih IM. 2011. ARID1A, a factor that promotes formation of SWI/SNF-mediated chromatin remodeling, is a tumor suppressor in gynecologic cancers. Cancer Res 71:6718-27.

8. Balm MN, Lee CK, Lee HK, Chiu L, Koay ES, Tang JW. 2012. A diagnostic polymerase chain reaction assay for Zika virus. J Med Virol 84:1501-5.

9. Chien LJ, Liao TL, Shu PY, Huang JH, Gubler DJ, Chang GJ. 2006. Development of real-time reverse transcriptase PCR assays to detect and serotype dengue viruses. J Clin Microbiol 44:1295-304.

10. Waggoner JJ, Rojas A, Mohamed-Hadley A, de Guillén YA, Pinsky BA. 2018. Real-time RT-PCR for Mayaro virus detection in plasma and urine. J Clin Virol 98:1-4.

11. Yang CF, De L, Yang SJ, Ruiz Gómez J, Cruz JR, Holloway BP, Pallansch MA, Kew OM. 1992. Genotype-specific in vitro amplification of sequences of the wild type 3 polioviruses from Mexico and Guatemala. Virus Res 24:277-96.

12. Zhou P, Yang XL, Wang XG, Hu B, Zhang L, Zhang W, Si HR, Zhu Y, Li B, Huang CL, Chen HD, Chen J, Luo Y, Guo H, Jiang RD, Liu MQ, Chen Y, Shen XR, Wang X, Zheng XS, Zhao K, Chen QJ, Deng F, Liu LL, Yan B, Zhan FX, Wang YY, Xiao GF, Shi ZL. 2020. A pneumonia outbreak associated with a new coronavirus of probable bat origin. Nature 579:270-273.

13. Rickard DJ, Sehon CA, Kasparcova V, Kallal LA, Zeng X, Montoute MN, Chordia T, Poore DD, Li H, Wu Z, Eidam PM, Haile PA, Yu J, Emery JG, Marquis RW, Gough PJ,

Bertin J. 2013. Identification of benzimidazole diamides as selective inhibitors of the nucleotide-binding oligomerization domain 2 (NOD2) signaling pathway. PLoS One 8:e69619.

14. Haile PA, Votta BJ, Marquis RW, Bury MJ, Mehlmann JF, Singhaus R, Charnley AK, Lakdawala AS, Convery MA, Lipshutz DB, Desai BM, Swift B, Capriotti CA, Berger SB, Mahajan MK, Reilly MA, Rivera EJ, Sun HH, Nagilla R, Beal AM, Finger JN, Cook MN, King BW, Ouellette MT, Totoritis RD, Pierdomenico M, Negroni A, Stronati L, Cucchiara S, Ziółkowski B, Vossenkämper A, MacDonald TT, Gough PJ, Bertin J, Casillas LN. 2016. The Identification and Pharmacological Characterization of 6-(tert-Butylsulfonyl)-N-(5-fluoro-1H-indazol-3-yl)quinolin-4-amine (GSK583), a Highly Potent and Selective Inhibitor of RIP2 Kinase. J Med Chem 59:4867-80.

15. Yin Z, Chen YL, Schul W, Wang QY, Gu F, Duraiswamy J, Kondreddi RR, Niyomrattanakit P, Lakshminarayana SB, Goh A, Xu HY, Liu W, Liu B, Lim JY, Ng CY, Qing M, Lim CC, Yip A, Wang G, Chan WL, Tan HP, Lin K, Zhang B, Zou G, Bernard KA, Garrett C, Beltz K, Dong M, Weaver M, He H, Pichota A, Dartois V, Keller TH, Shi PY. 2009. An adenosine nucleoside inhibitor of dengue virus. Proc Natl Acad Sci U S A 106:20435-9.

16. Pruijssers AJ, George AS, Schäfer A, Leist SR, Gralinksi LE, Dinnon KH, Yount BL, Agostini ML, Stevens LJ, Chappell JD, Lu X, Hughes TM, Gully K, Martinez DR, Brown AJ, Graham RL, Perry JK, Du Pont V, Pitts J, Ma B, Babusis D, Murakami E, Feng JY, Bilello JP, Porter DP, Cihlar T, Baric RS, Denison MR, Sheahan TP. 2020. Remdesivir Inhibits SARS-CoV-2 in Human Lung Cells and Chimeric SARS-CoV Expressing the SARS-CoV-2 RNA Polymerase in Mice. Cell Rep 32:107940.

17. Hou S, Kumar A, Xu Z, Airo AM, Stryapunina I, Wong CP, Branton W, Tchesnokov E, Götte M, Power C, Hobman TC. 2017. Zika Virus Hijacks Stress Granule Proteins and Modulates the Host Stress Response. J Virol 91.

FIG S1

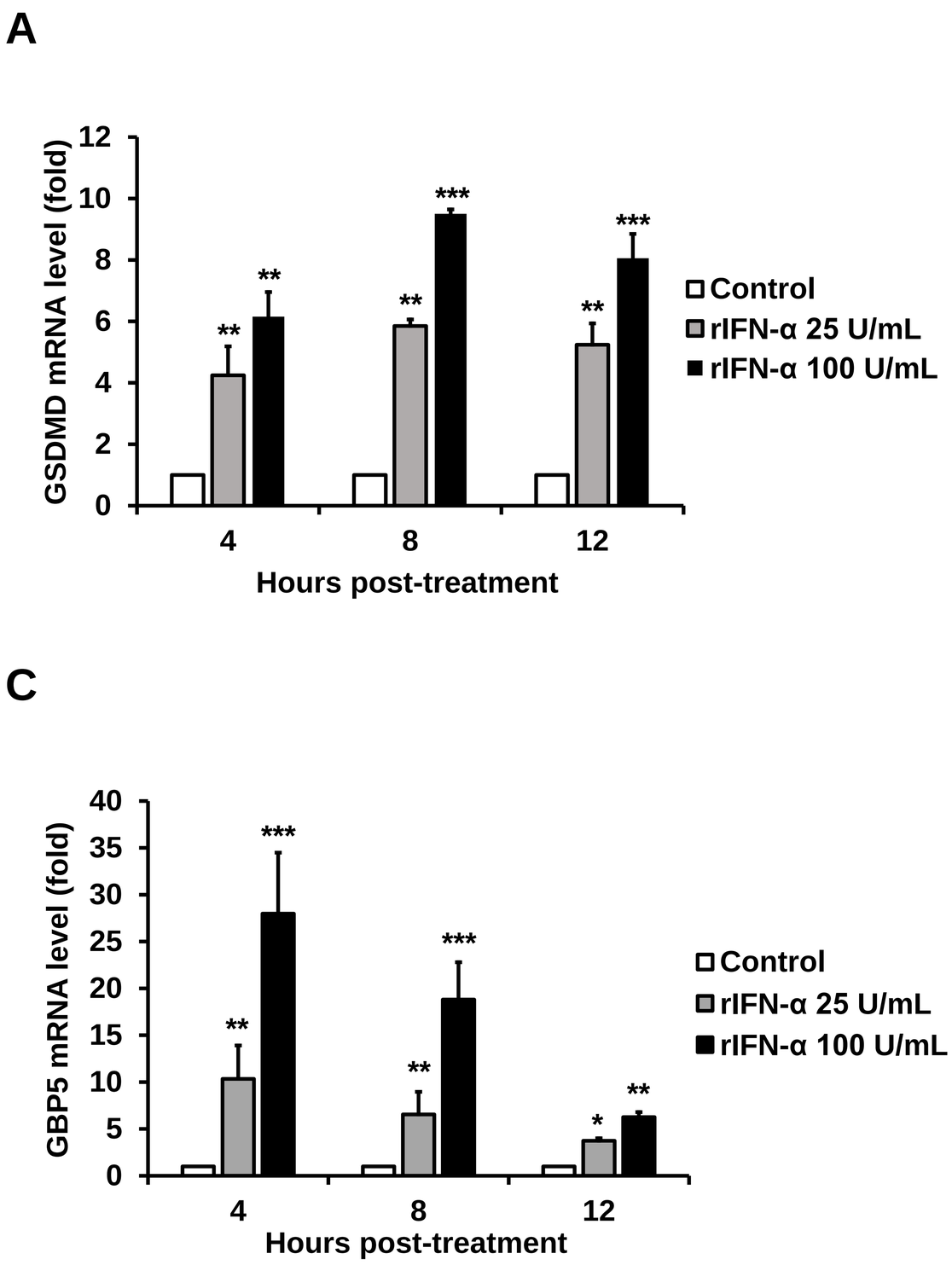
A
GSDMD mRNA level (fold)
0
2
4
6
8
10
12
**
**
**
***
**
***
4
8
12
Hours post-treatment
Control
rIFN-α 25 U/mL
rIFN-α 100 U/mL

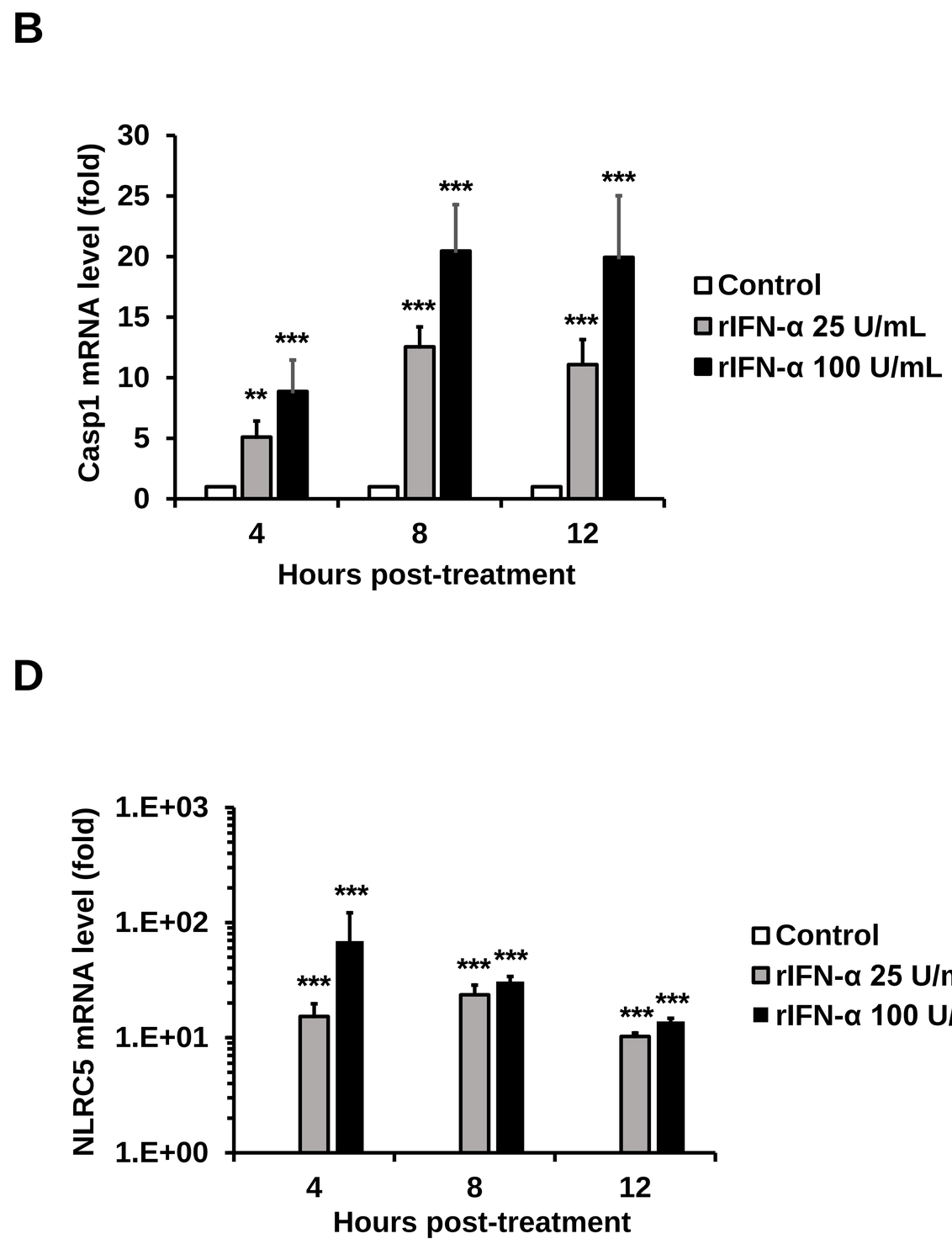
B
Casp1 mRNA level (fold)
0
5
10
15
20
25
30
**
***
***
***
***
***
4
8
12
Hours post-treatment
Control
rIFN-α 25 U/mL
rIFN-α 100 U/mL

C
GBP5 mRNA level (fold)
0
5
10
15
20
25
30
35
40
**
***
**
***
*
**
4
8
12
Hours post-treatment
Control
rIFN-α 25 U/mL
rIFN-α 100 U/mL

D
NLRC5 mRNA level (fold)
1.E+00
1.E+01
1.E+02
1.E+03
***
***
***
***
***
***
4
8
12
Hours post-treatment
Control
rIFN-α 25 U/mL
rIFN-α 100 U/mL

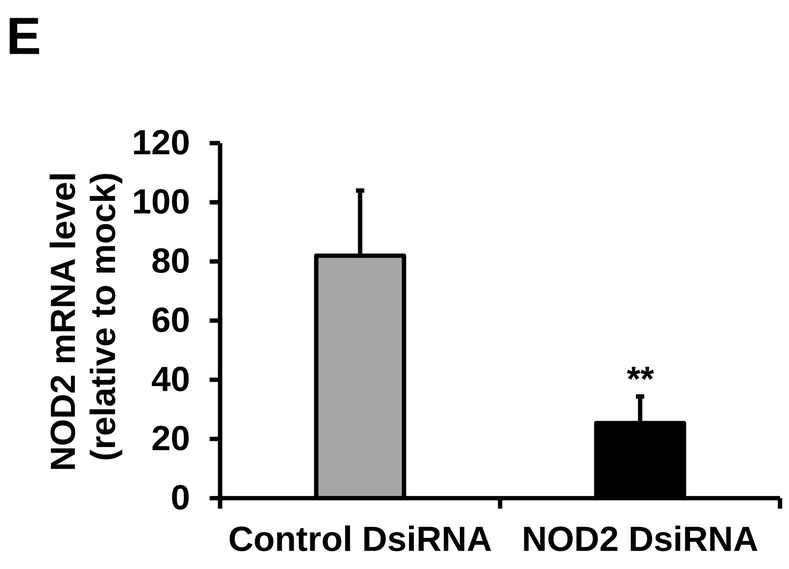
E
NOD2 mRNA level
(relative to mock)
0
20
40
60
80
100
120
**
Control DsiRNA
NOD2 DsiRNA

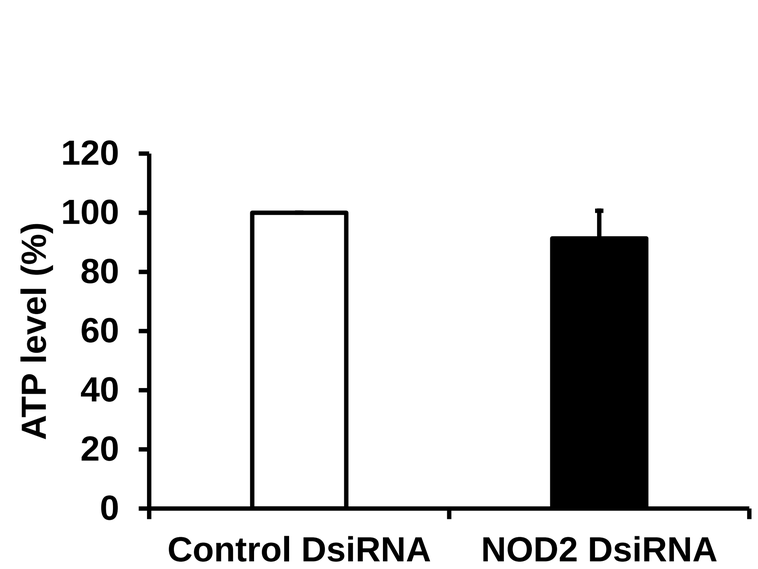
F
ATP level (%)
0
20
40
60
80
100
120
Control DsiRNA
NOD2 DsiRNA

FIG S2

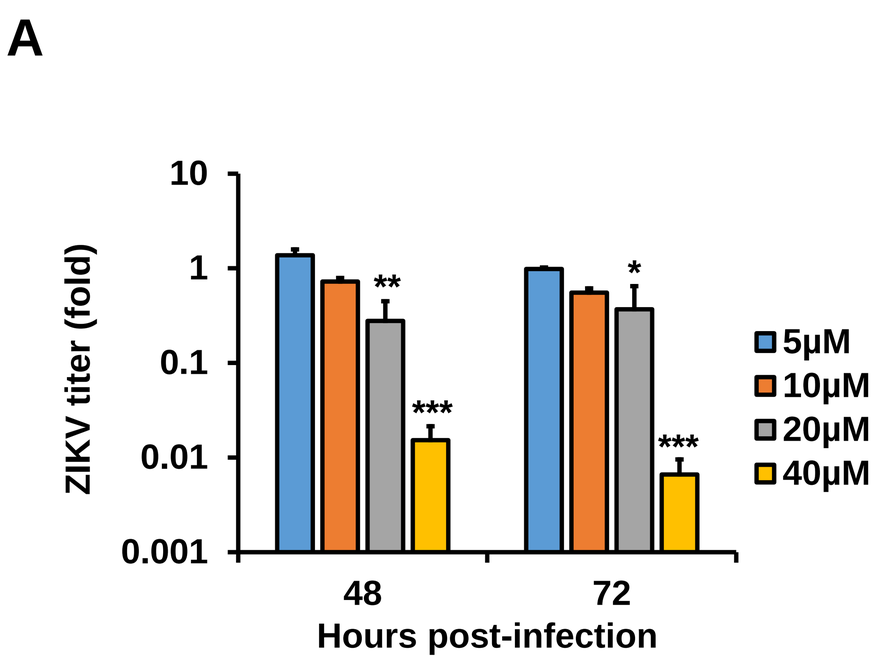
A
ZIKV titer (fold)
10
1
0.1
0.01
0.001
**
*
***
***
48
72
Hours post-infection
5μM
10μM
20μM
40μM

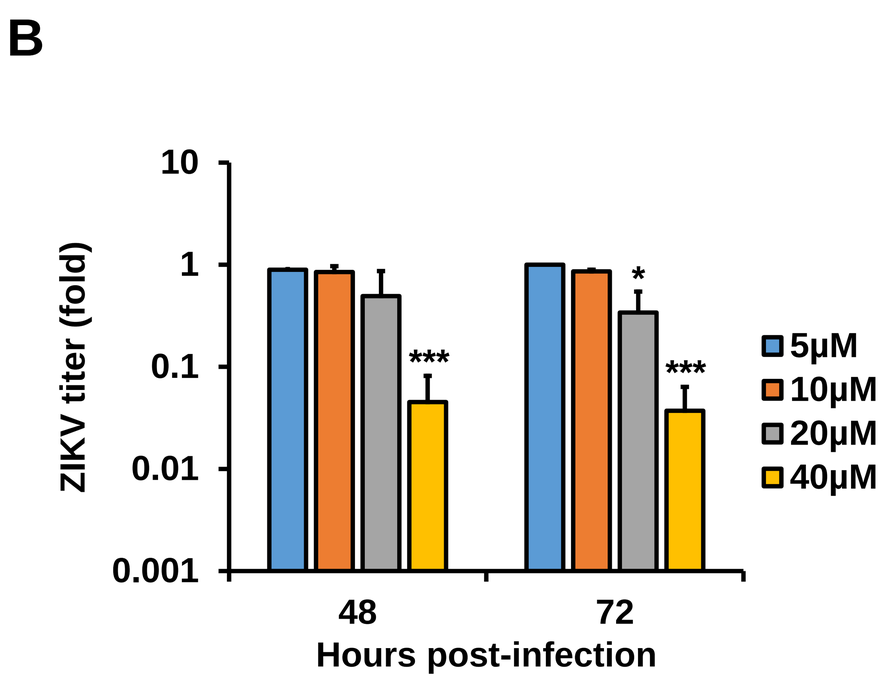
B
ZIKV titer (fold)
10
1
0.1
0.01
0.001
***
*
***
48
72
Hours post-infection
5μM
10μM
20μM
40μM

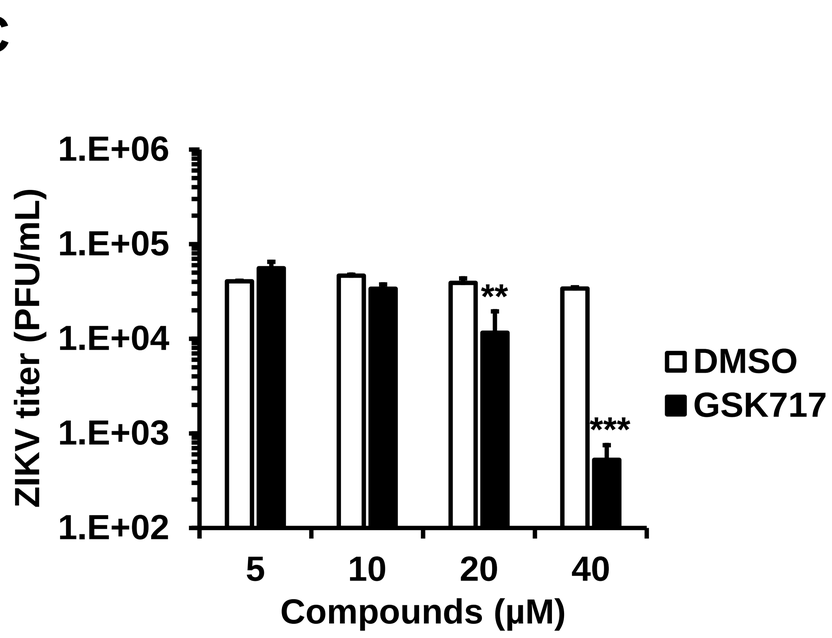
C
ZIKV titer (PFU/mL)
1.E+06
1.E+05
1.E+04
1.E+03
1.E+02
**
***
5
10
20
40
Compounds (μM)
DMSO
GSK717

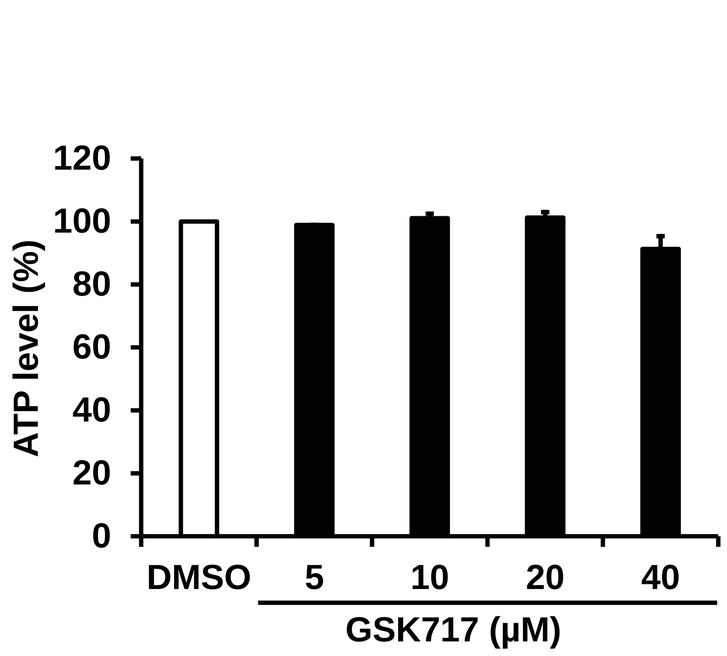
D
ATP level (%)
120
100
80
60
40
20
0
DMSO
5
10
20
40
GSK717 (μM)

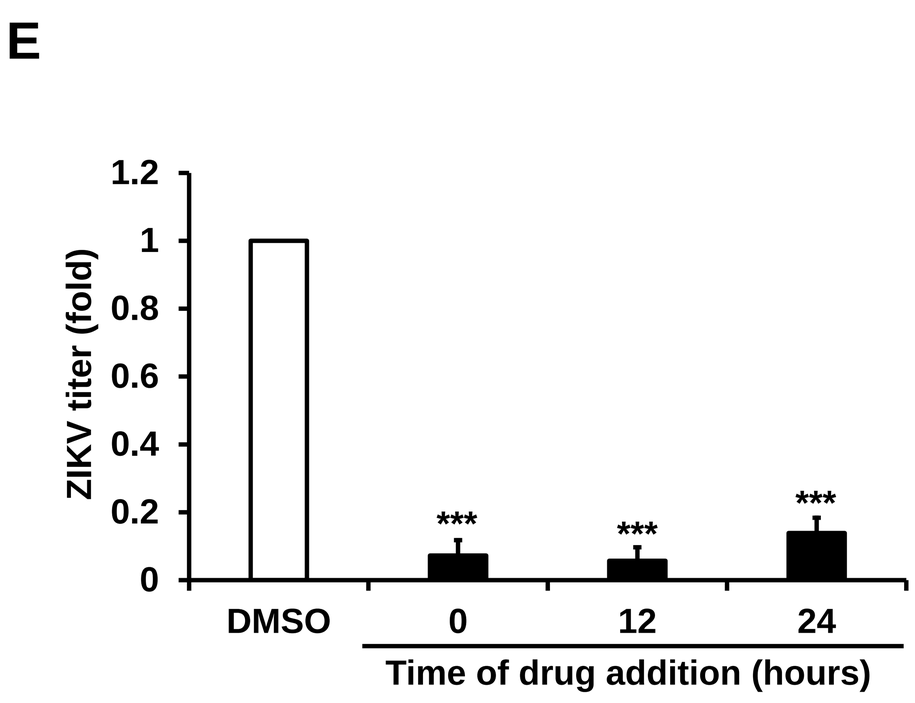
E
ZIKV titer (fold)
1.2
1
0.8
0.6
0.4
0.2
0
***
***
***
DMSO
0
12
24
Time of drug addition (hours)

FIG S3

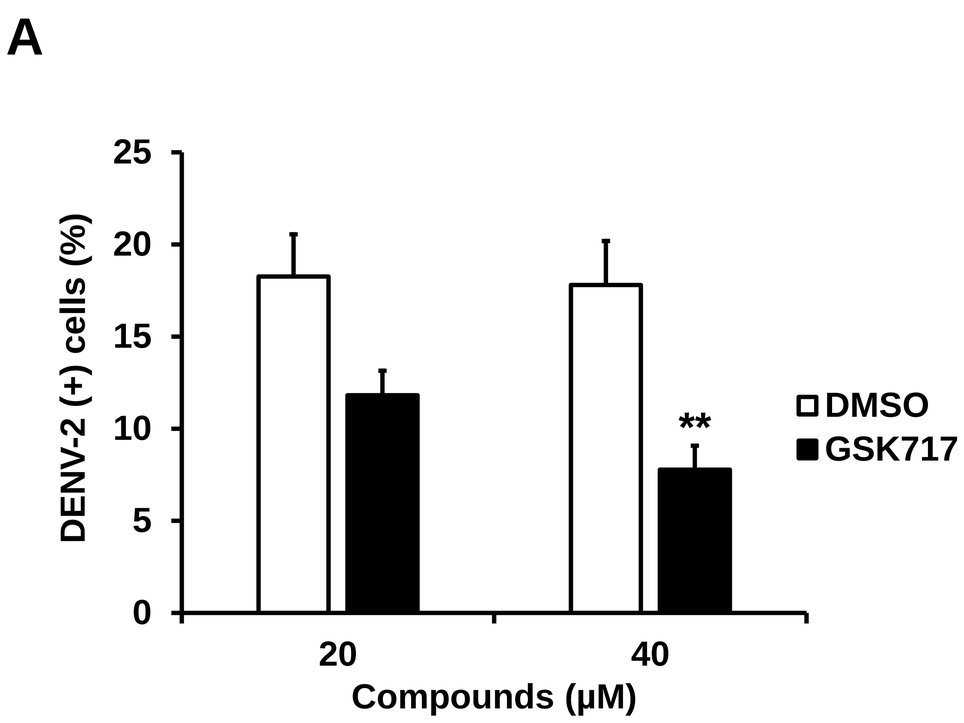
A
25
20
15
10
5
0
DENV-2 (+) cells (%)
**
DMSO
GSK717
20
40
Compounds (μM)

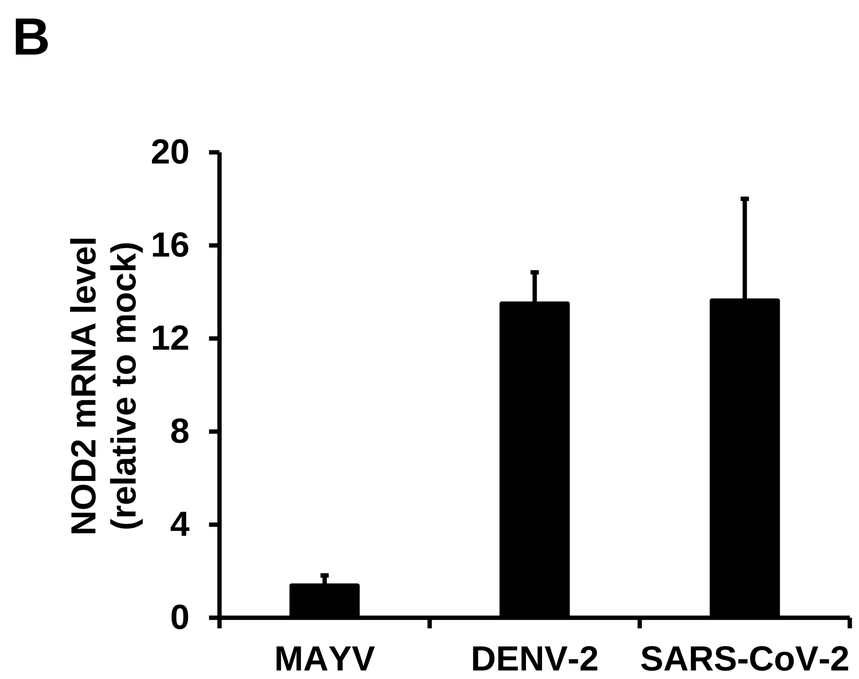
B
20
16
12
8
4
0
NOD2 mRNA level
(relative to mock)
MAYV
DENV-2
SARS-CoV-2

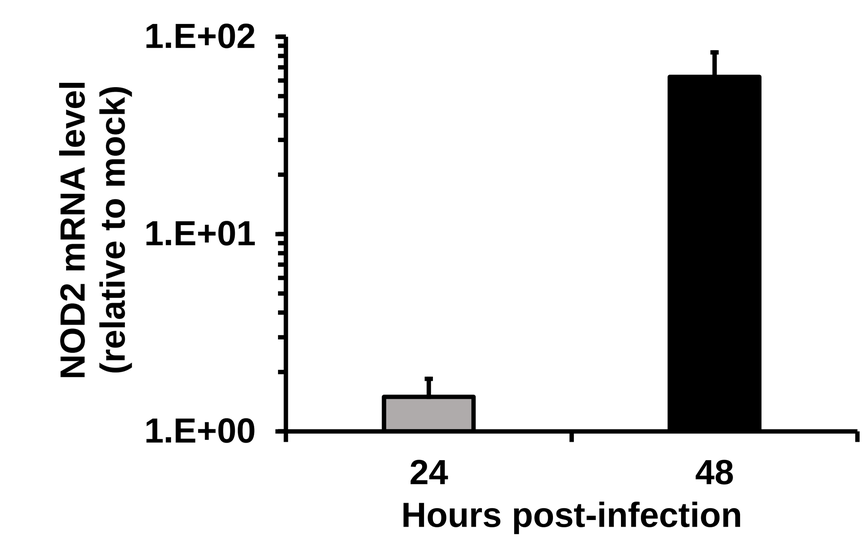
C
1.E+02
1.E+01
1.E+00
NOD2 mRNA level
(relative to mock)
24
48
Hours post-infection

FIG S4

A


0.25
0.2
0.15
0.1
0.05
0
MAYV titer (fold)
***
***
12
24
Time post-infection (hours)

B

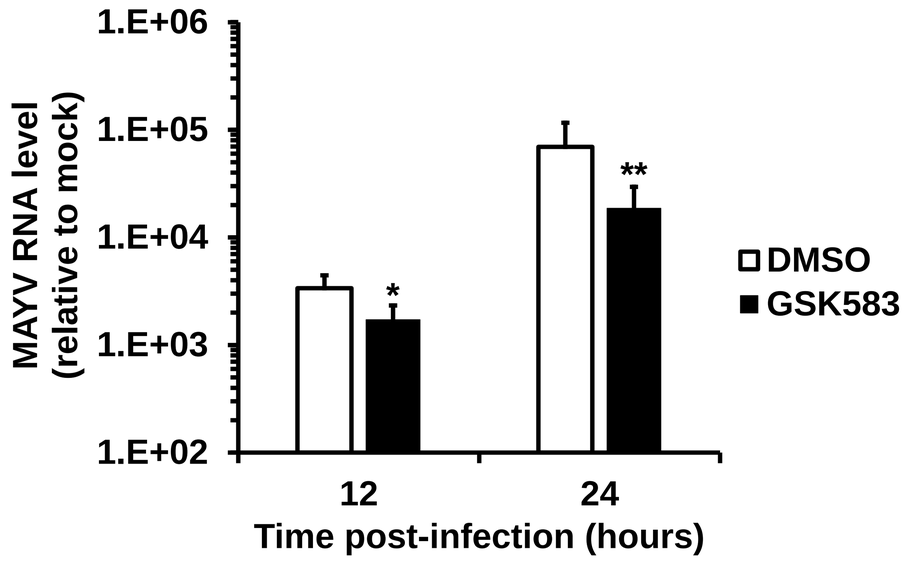
1.E+06
1.E+05
1.E+04
1.E+03
1.E+02
MAYV RNA level
(relative to mock)
*
**
DMSO
GSK583
12
24
Time post-infection (hours)

C

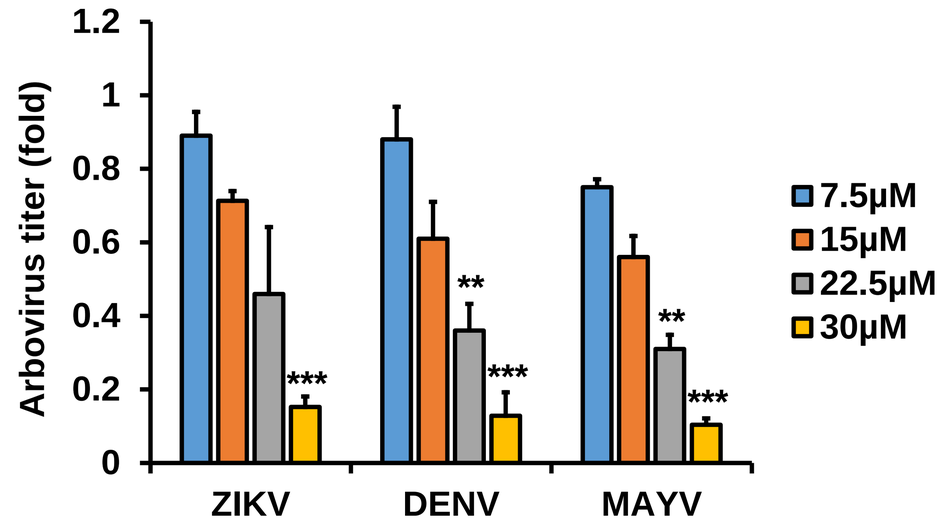
1.2
1
0.8
0.6
0.4
0.2
0
Arbovirus titer (fold)
**
***
7.5μM
15μM
22.5μM
30μM
ZIKV
DENV
MAYV

D

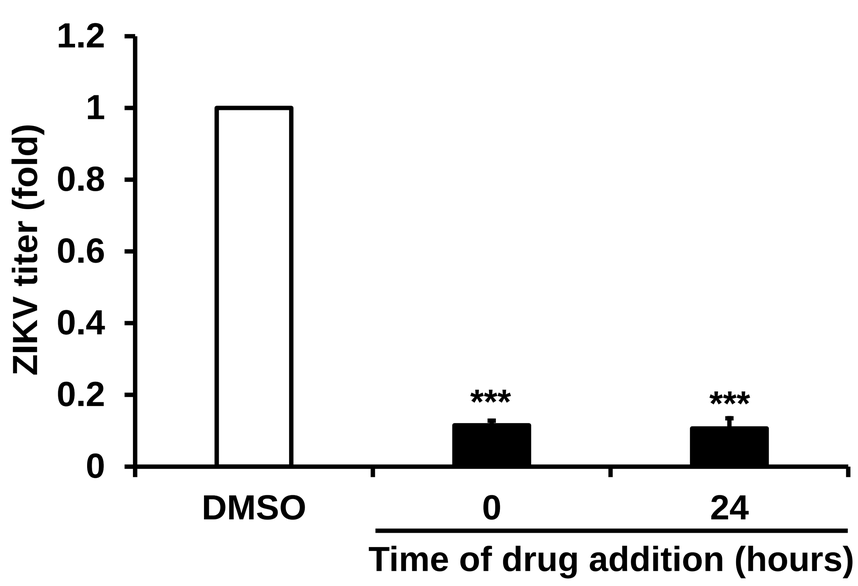
1.2
1
0.8
0.6
0.4
0.2
0
ZIKV titer (fold)
***
***
DMSO
0
24
Time of drug addition (hours)

E

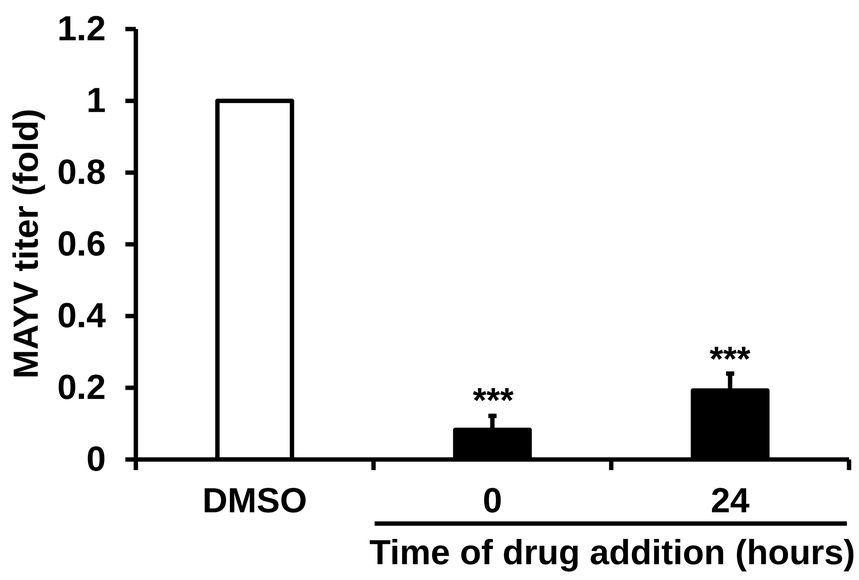
1.2
1
0.8
0.6
0.4
0.2
0
MAYV titer (fold)
***
***
DMSO
0
24
Time of drug addition (hours)

FIG S5

A

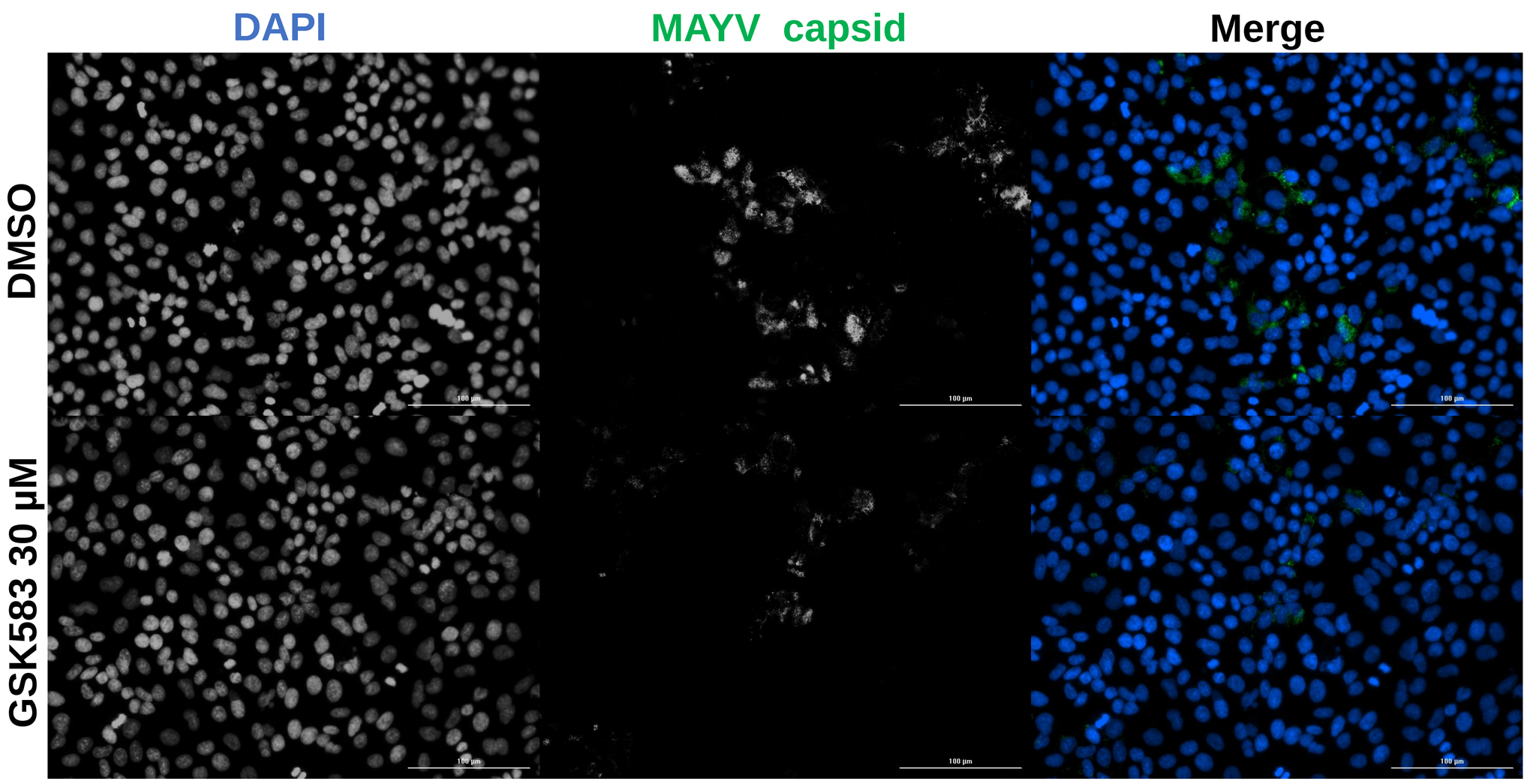
DAPI
MAYV capsid
Merge
DMSO
GSK583 30 μM
100 μm

B

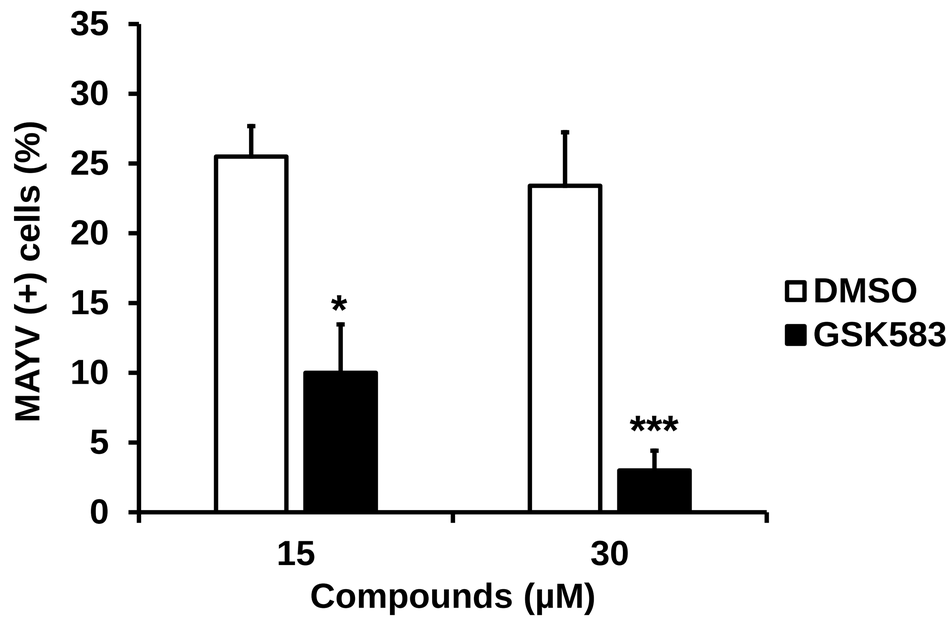
MAYV (+) cells (%)
35
30
25
20
15
10
5
0
*
***
15
30
Compounds (μM)
DMSO
GSK583

C

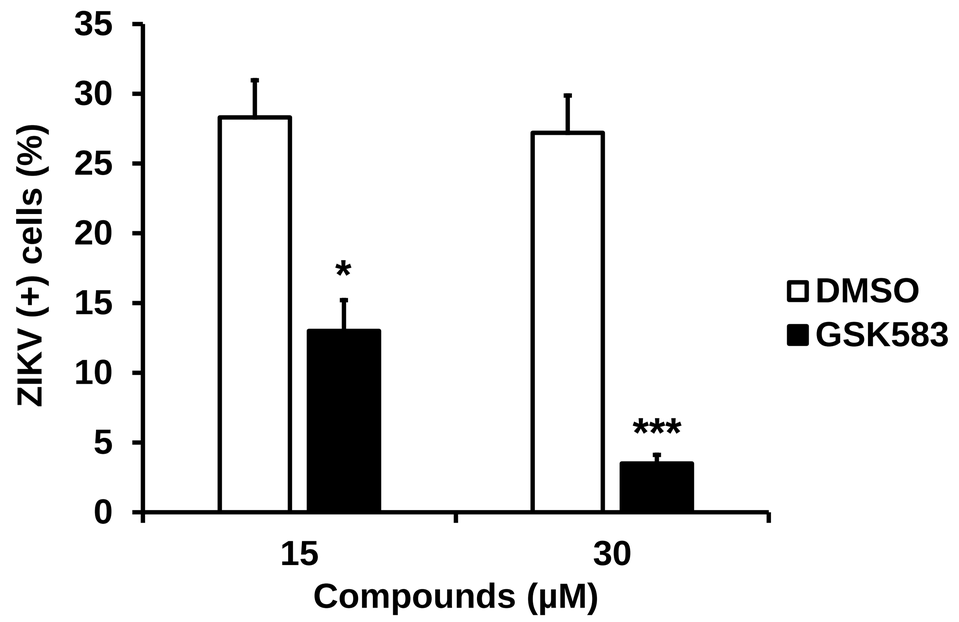
ZIKV (+) cells (%)
35
30
25
20
15
10
5
0
*
***
15
30
Compounds (μM)
DMSO
GSK583

D

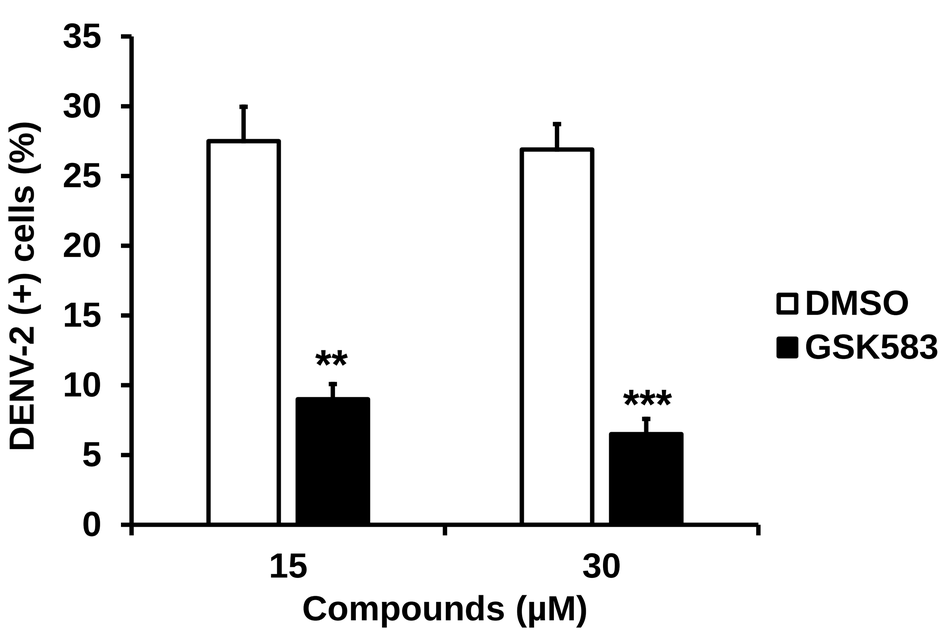
DENV-2 (+) cells (%)
35
30
25
20
15
10
5
0
**
***
15
30
Compounds (μM)
DMSO
GSK583

F

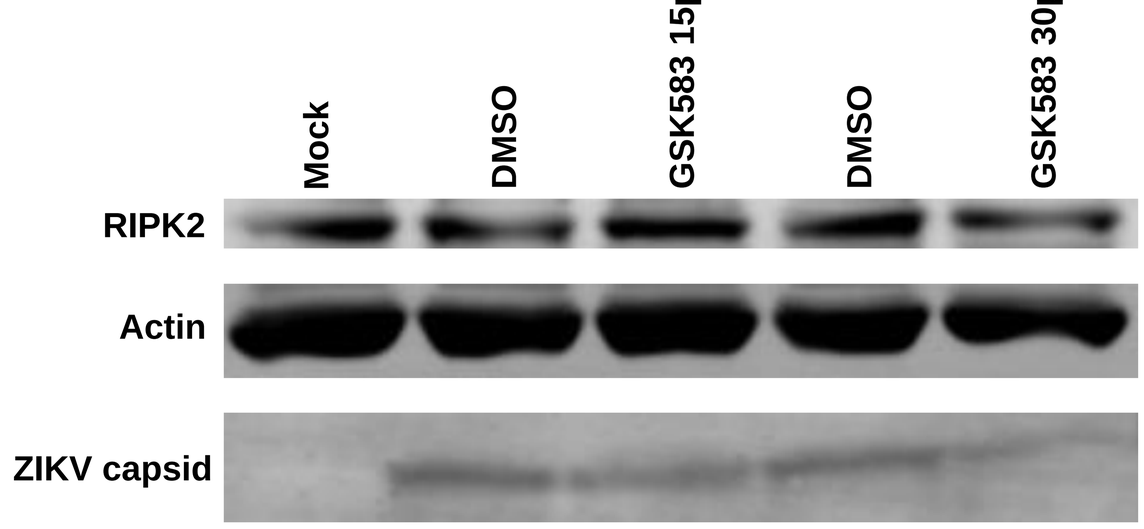
Mock
DMSO
GSK583 15μM
DMSO
GSK583 30μM
RIPK2
Actin
ZIKV capsid

FIG S6

A

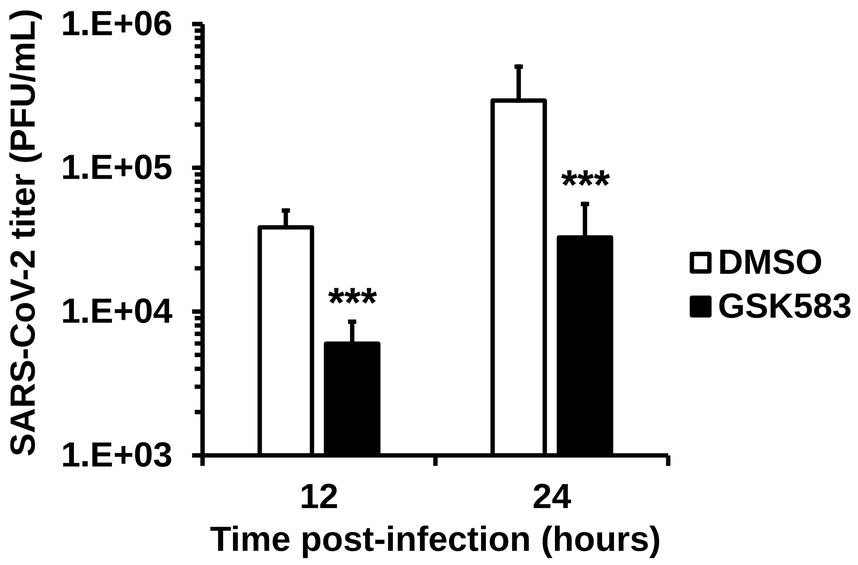
SARS-CoV-2 titer (PFU/mL)
1.E+06
1.E+05
1.E+04
1.E+03
***
***
DMSO
GSK583
12
24
Time post-infection (hours)

B

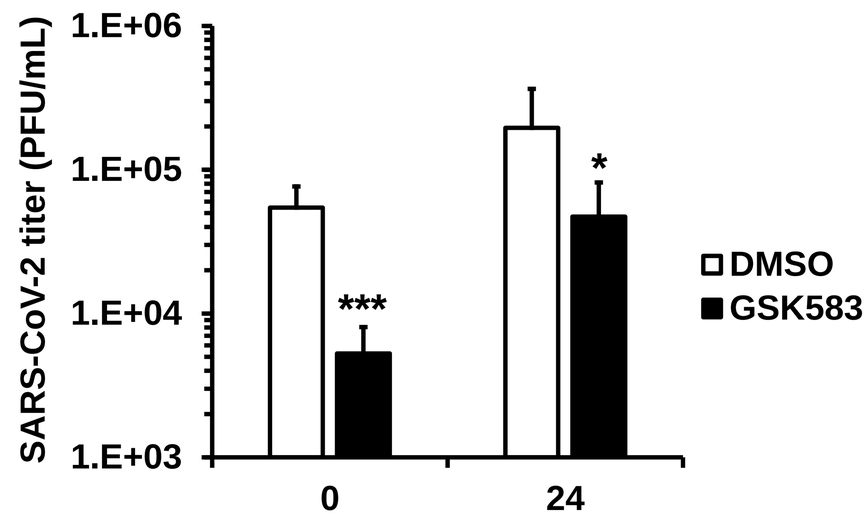
SARS-CoV-2 titer (PFU/mL)
1.E+06
1.E+05
1.E+04
1.E+03
***
*
DMSO
GSK583
0
24
Time of drug addition (hours)

C

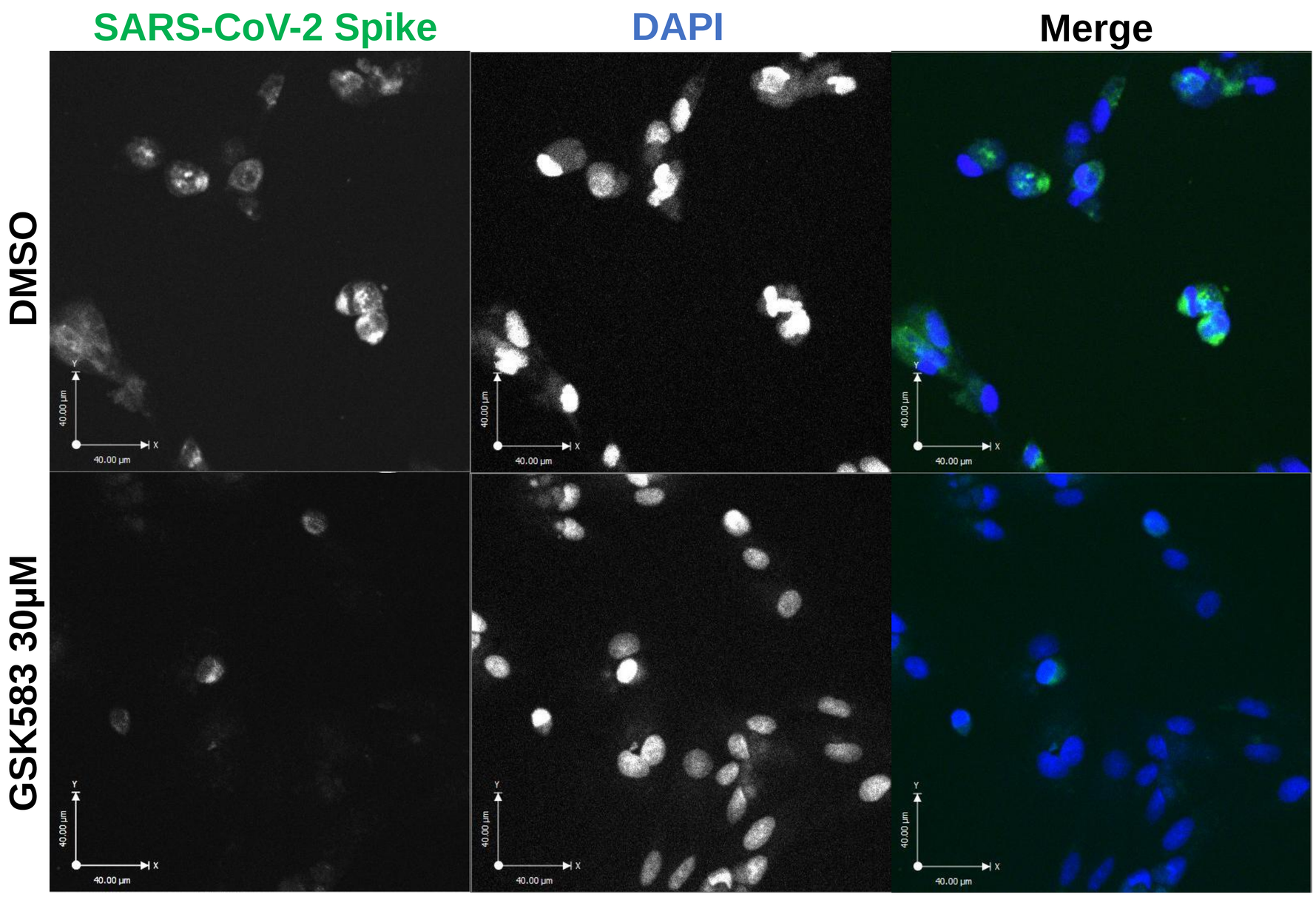
SARS-CoV-2 Spike
DAPI
Merge
DMSO
GSK583 30μM
40.00 μm

D

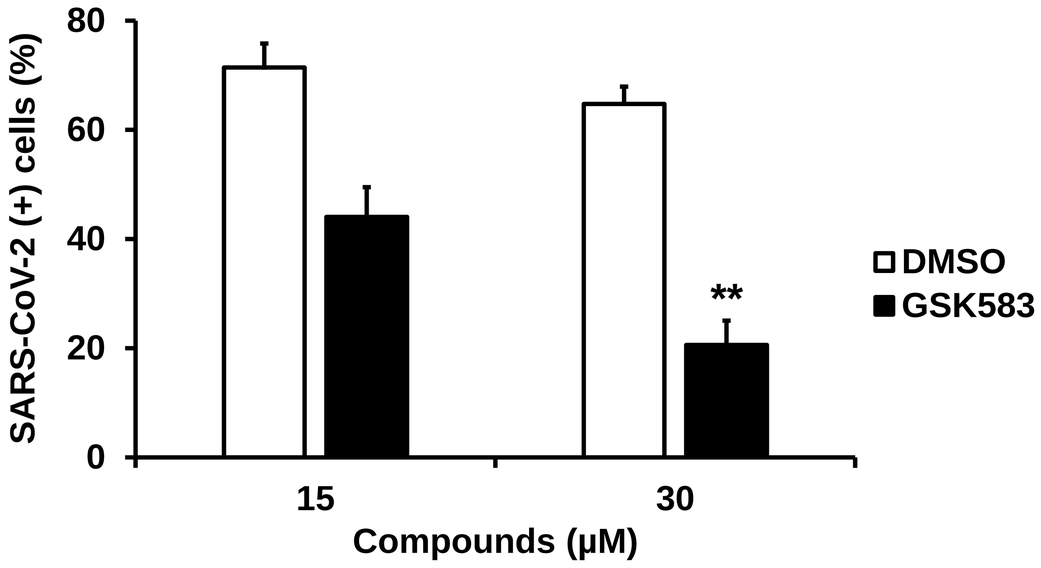
SARS-CoV-2 (+) cells (%)
80
60
40
20
0
**
DMSO
GSK583
15
30
Compounds (μM)

FIG S7

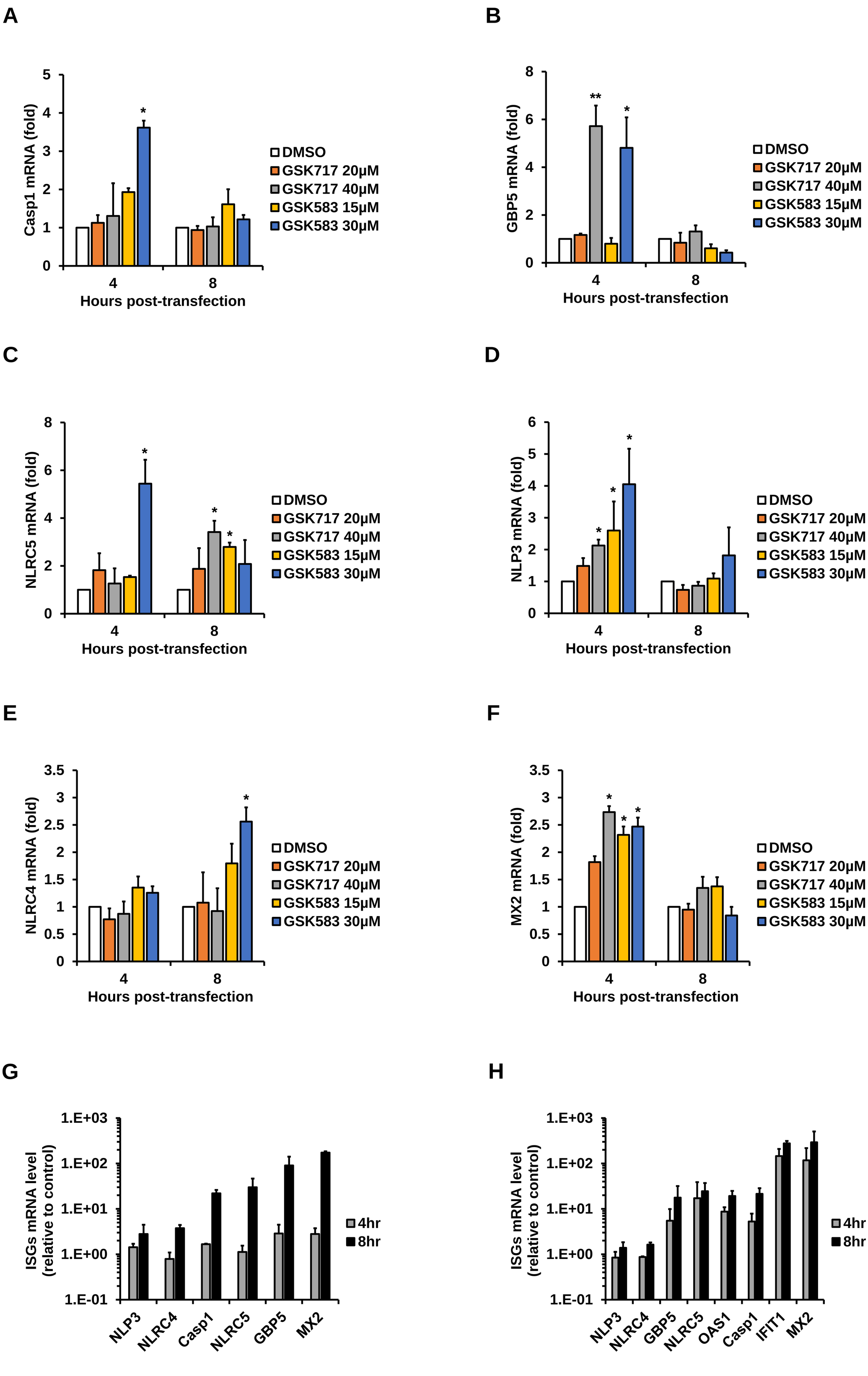
A
Casp1 mRNA (fold)
Hours post-transfection
DMSO
GSK717 20μM
GSK717 40μM
GSK583 15μM
GSK583 30μM
B
GBP5 mRNA (fold)
C
NLRC5 mRNA (fold)
D
NLP3 mRNA (fold)
E
NLRC4 mRNA (fold)
F
MX2 mRNA (fold)
G
ISGs mRNA level (relative to control)
4hr
8hr
NLP3
NLRC4
Casp1
NLRC5
GBP5
MX2
H
OAS1
IFIT1